

# Critical conditions for failure; stress levels, length scales, time scales

**DOI:**[10.1063/1.4971631](https://doi.org/10.1063/1.4971631)**Document Version**

Final published version

[Link to publication record in Manchester Research Explorer](#)**Citation for published version (APA):**

Bourne, N., Gray III, C. T., & Bronkhorst, C. A. (2017). Critical conditions for failure; stress levels, length scales, time scales. In *SHOCK COMPRESSION OF CONDENSED MATTER : Proceedings of the Conference of the American Physical Society Topical Group on Shock Compression of Condensed Matter 2015* (Vol. 1793). American Institute of Physics. <https://doi.org/10.1063/1.4971631>

**Published in:**

SHOCK COMPRESSION OF CONDENSED MATTER

**Citing this paper**

Please note that where the full-text provided on Manchester Research Explorer is the Author Accepted Manuscript or Proof version this may differ from the final Published version. If citing, it is advised that you check and use the publisher's definitive version.

**General rights**

Copyright and moral rights for the publications made accessible in the Research Explorer are retained by the authors and/or other copyright owners and it is a condition of accessing publications that users recognise and abide by the legal requirements associated with these rights.

**Takedown policy**

If you believe that this document breaches copyright please refer to the University of Manchester's Takedown Procedures [<http://man.ac.uk/04Y6Bo>] or contact [uml.scholarlycommunications@manchester.ac.uk](mailto:uml.scholarlycommunications@manchester.ac.uk) providing relevant details, so we can investigate your claim.



## Critical conditions for failure; stress levels, length scales, time scales

N. K. Bourne, G. T. GrayIII, and C. A. Bronkhorst

Citation: **1793**, 100006 (2017); doi: 10.1063/1.4971631

View online: <http://dx.doi.org/10.1063/1.4971631>

View Table of Contents: <http://aip.scitation.org/toc/apc/1793/1>

Published by the [American Institute of Physics](#)

---

---

# Critical Conditions for Failure; Stress Levels, Length Scales, Time Scales

N.K. Bourne<sup>1 a)</sup>, G.T. Gray III<sup>2</sup>, C.A. Bronkhorst<sup>2</sup>

<sup>1</sup>*School of Materials, University of Manchester, Rutherford Appleton Laboratory, Didcot, Oxfordshire, OX11 0FA.*

<sup>2</sup>*Los Alamos National Laboratory, Los Alamos, NM, USA.*

<sup>a)</sup>Corresponding author: neil.bourne@manchester.ac.uk

**Abstract.** There is a range of thresholds for the response of condensed matter under loading in compression, from the yield point to that at which the bond strength is overcome and warm dense matter is formed. Yield stress shows a correlation between the length scale swept by the rise of the pulse and the defect distribution within the target for a range of materials. Strain rate is also a useful term that reflects the evolution of the stress state within a target but must also be defined for a volume element containing a particular defect distribution to reflect continuum conditions acting within; it thus applies to a defined length scale within a target. Examples are shown using shock pulses that spall metal targets. Different stacking shows differing behaviour yet in each case momentum is conserved. This overview suggests simple observations must take account of mechanisms operating at different timescales and lengthscales in the development of damage in materials and structures.

## 1. INTRODUCTION

The systematic investigation of material deformation was first prompted by the need (and indeed the continuing need) to describe materials' failure. Early inputs to the field came via developments in solid mechanics through the 19th century [1, 2]. Advances in experiment and observation, particularly from developing heavy industry, showed that localization of deformation was a key feature of response [3]. One principal requirement for stronger and more durable metals came from military requirements for better performance in ever more demanding environments [4]. One realization was that in order to advance, the field must consider loading on the materials and structures that was not gradual but driven by impulses from impact or explosion [4]. Early investigators of dynamic failure were John and Bertram Hopkinson who found methods to induce tensile failure under impulsive loading [5]. In this spirit, this paper discusses dynamic failure or spallation in metals to review understanding of the response of materials to tensile impulse.

Loading may in general be decomposed into components of compression, tension or torsion to describe the means by which a material accommodates an applied strain (in impact the stress results from an applied strain). It is useful to classify the physical mechanisms that give rise to dynamic tensile failure into three groups illustrated in Fig. 1. The first (1 a) is a one-dimensional uniaxial tensile strain resulting from the interaction of two release fans from compressive wave loading. A second failure mode (1 b) results from wave reflection of a triangular wave from an interface with a lower impedance material beyond (the magnitude of that reflection is maximized if the surface is free). In the final scenario (1 c), metal is failed in a two-dimensional loading where a cylindrical metal shell is ruptured by hoop stresses generated by expansion of the case.

In the majority of situations, a dynamic tensile impulse results from a wave interaction that occurs within a target so that a material experiences dynamic tension *after* it has been previously compressed. This work will thus address loading in one-dimension (at the macroscale at least) where mechanisms and their development can be most rigorously investigated. What will become clear is that understanding is much less developed for this mode of loading than is the case for compression and the analytical framework that exists to describe it is largely empirical. Further, numerical modeling is also problematic since compression homogenizes inhomogeneous response whereas tensile failure localizes it at a series of structural defects such that continuum codes with ideal meshes cannot easily account for the failure.

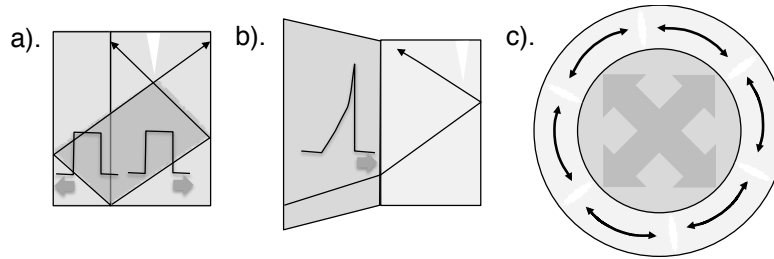


**FIGURE 1.** Modes of dynamic tensile failure; a). one-dimensional by wave interaction, b). one-dimensional wave reflection, c). two-dimensional expansion with circumferential tension.

When matter begins to deform under a stress that exceeds the yield strength, it fails at its weakest point and localises at its largest defect. If the material has multiple phases this process continues over a transition range of stresses and strains as each phase within the microstructure fails. Component scale uniaxial loading will localise into a fully three dimensional field at the scale beneath the one probed so that failure at defects will start in all cases. In a state of macroscopic tension, bonds are broken in tension or shear defining the mesoscale and new surfaces are created within the strained volume probed. At the micro- or nanoscale, within a grain of material with no volume defects, forces are electrostatic and tensile strength is markedly higher than within the bulk. At the mesoscale and greater, failure is generally by fracture or cavitation determined again by longer-range bond strength and stacking within the microstructure. Here materials with low Peierls stress can readily deform by slip and cavitate at inhomogeneities in the manner of bubbles forming within liquids.

In the ideal case a material would fail in tension at its theoretical tensile strength. There are various forms one could take for calculating such a value according to assumptions about the potential that governs the electronic state in the material. If one were to approximate the interatomic force with a simple sine function then the critical stress might be represented in the following manner

$$\sigma = \sigma_T \sin\left(\frac{2\pi x}{a}\right) = \sigma_T \sin(2\pi\varepsilon) \Rightarrow \sigma_T = \frac{E}{2\pi}. \quad (1)$$

where  $\sigma_T$  is the tensile strength,  $\varepsilon$  is the strain and  $E$  is the Young's modulus. It is well known that this value is much greater than those measured. For a metal like pure copper for example, the Young's modulus is *ca.* 130 GPa which gives a value for the theoretical tensile strength of *ca.* 20 GPa. In dynamic experiments on the same metal (using plate impact) *ca.* 1.5 GPa is measured. This value is about 3% of the theoretical strength. In general terms, the theoretical strength of metals is around ten times, and in that of brittle materials one hundred times the observed values [6]. Analysis of theoretical strength makes the key assumption that the bonding in matter at every scale is electrostatic and that this must be overcome by the forces that result from the loading impulse. In the weak shock regime the strength is not controlled by valence-electron bonding since within the material the strain induced spans joints which are much weaker and fail rapidly under tensile load. Only in the strong shock regime is bonding in the region where the materials failure is described purely by the atomic potential.

In loading of materials and structures at the laboratory scale, the volumes loaded include meso- and component scales where amorphous stacking or joints control bonding. In these cases failure is always at a length scale and a stress amplitude that is very much less than the theoretical limit. It is only when short duration impulses are applied to materials that the volume elements probed are sufficiently small that theoretical strength might be attained. Between the yield surface and the theoretical strength, smaller defects are activated and slip initiated at deformation planes so that elastic blocks slip on active planes. As stress levels increase all defects become activated until the theoretical strength (overdrive from weak to strong shock at the Weak Shock Limit; WSL in shocked solids [6, 7]) is reached and material flows in a homogeneous hydrodynamic state. However the regimes up to the point at which theoretical strength is passed are controlled by defects within the microstructure and tensile behaviour has been measured with impulses of varying nature that we reviewed below.

## 2. MATERIAL RESPONSE IN DIFFERENT REGIMES OF BEHAVIOUR

### 2.1 Behaviour in compression

This review considers behaviour under loading by impulses that apply net tension to a region within a material, but the previous section has made it clear that it is rarely the case that a volume element experiences tension without

having just been released from a state of compression. The effects of a tensile pulse depend upon the nature of the solid that experiences the impulse. In the case of crystalline solids, stacking dictates the Peierls stress and this determines the ease of nucleation and propagation of slip in the material. If this quantity is high, slip is difficult and thus hardening by dislocation interaction and entanglement during pulse propagation is difficult. Thus, precompression and release change the microstructure by a small amount insufficient to affect the bulk properties that result in such a material. If the Peierls stress is low however, the ease of dislocation nucleation and propagation mean that flow and dislocation tangling may occur on the timescales of an impulse thereby hardening the material and increasing the strength seen on release and after subsequent tensile loading. Accordingly, preconditioning by a compression pulse may have a significant effect upon the tensile strength that results. A second feature that determines the ease of flow is the stacking fault energy (SFE). High SFE in metals results in the material deforming easily by dislocation glide. Low SFE materials have difficulties in cross-slip and climb making cross-slip harder. In this case a material is more likely to twin rather than slip and the yield stress of the target is higher than equivalent materials. Of course a high precompression may trigger martensitic phase transformation instead. In materials with restricted slip planes, plasticity within grains is then generally more difficult than failure of grain boundaries by fracture. This is typically the case in ceramics for instance.

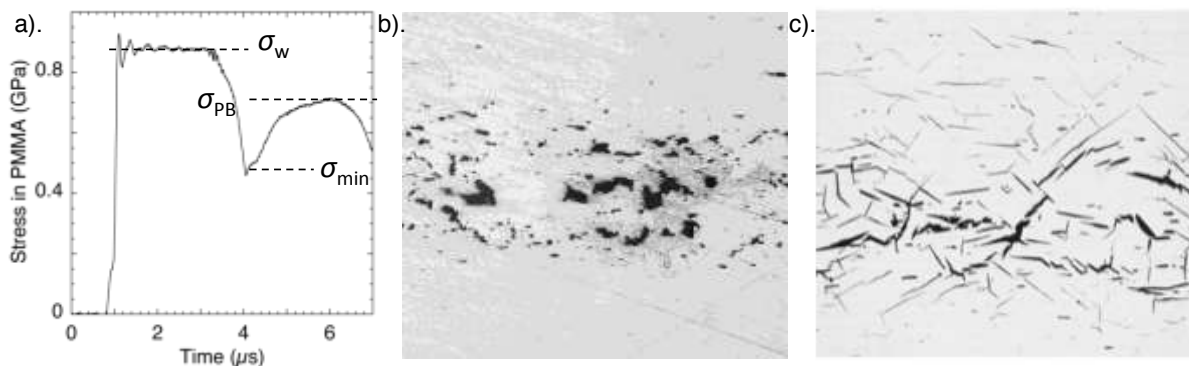


**FIGURE 2.** Spall in XM copper (a). stress history at window and microstructure of opened plane b). c). failure in ARMCO iron [10];  $\sigma_w$  is stress at PMMA window,  $\sigma_{min}$  stress after first release,  $\sigma_{PB}$  pull back stress.

There are thus two general modes of failure within materials loaded at scales that span a distance greater than a single grain; fracture or void growth. Fracture is favoured within the grain boundaries at the mesoscale when slip is difficult and void growth can again be triggered at this larger scale when it is not. Short pulses probe short distances and allow only mechanisms with fast kinetics to occur. Thus ductile void growth is a process that starts with local shear on easy planes followed by the opening and coalescence of plane surfaces along these directions. Development of ductile fractures into spherical (generally elliptical) voids occurs at later time when the process is controlled by the flow within the material, material density (due to inertial effects) and surface tension in the void when scales have moved beyond those of a single grain. Thus a transition in mechanisms is seen between short pulses (*e.g.* laser shock) and longer pulses (*e.g.* flyer plate) loadings from fracture to ductile void growth (see Fig. 2). Such a transition may appear to be a classic brittle-ductile transition but in fact is a function of the kinetics of processes activated and of the defect structures in the regions sampled by the pulses. This will be illustrated below for spall strength measurements in aluminium [7].

We shall principally consider ductile void growth in high SFE metals here to illustrate the points made in the preceding sections and use these behaviours to analyse response further to the impulses discussed above. Nevertheless the principles apply to all classes of material and note will be made in particular cases of these differences below.

## 2.2 Nucleation in tension

Cavitation in liquids can be induced by boiling or mechanical tensile loading. Such cavitation is seen to form in two modes in which either failure is immediate and forms sheets or develops from nuclei to form bubbles; homogeneous and heterogeneous nucleation respectively [8]. The latter proceeds by nucleation at inhomogeneities; defects on the surface of the liquid enclosure such as scratches or particles of dust entrained within the fluid. Homogeneous nucleation is the failure of the liquid that opens a new free surface within the material under load. In

this case failure occurs in sheets at higher flow rates and may be seen in fluid flow over aerofoils [8]. In the case of heterogeneous bubble formation in free fields within a liquid, the bubble sizes observed have dimensions ranging from *ca.* 1  $\mu\text{m}$  in cavitated seawater to *ca.* 100 nm in laser shocked fluids. Other shock experiments on fluids have reported measured liquid strengths which approach the homogeneous cavitation limit in the fluid as the shock amplitude increases and the pulse length under compression is reduced [9]. In shock loading, a simple way to change the duration of the impulse is to vary the input compression pulse by using different loading platforms. Laser pulses load for *ca.* 1 ns, explosive pulses for *ca.* 50 ns and a typical impacting plate for *ca.* 1  $\mu\text{s}$ . The loading pulse time decreases in each case with the highest strength recorded for a triangular pulse which samples a smaller volume of defect particles within a fluid. This trend will continue until the limiting cavitation strength of the fluid will be found at the bond strength between molecules. These features of tensile failure in a liquid can be extended to the response of ductile metals.

When liquids fail at inhomogeneities, spherical cavities will be almost instantaneously formed once the Van de Waals bonds between molecules are broken. However the first moments of failure in a solid will be down planes located around a defect and only when free surfaces have been opened and bonding is reduced will cavities start to form. The defect formed at these early stages is at the microscale within the solid under load. Since deformation processes are sequential and strain naturally builds, the transition from fracture to cavitation in solids takes time and this may be interrogated by varying pulse length and observing changes in failure mode at the mesoscale.

When a cavity is formed and other bonds are broken, the free surface created has a critical energy associated with it. This critical condition for flaw propagation is such that the work done at a flaw must exceed the surface energy for it to grow. Below this critical size there is not enough energy deposition to create a propagating void. That condition would have a stress  $\sigma$  acting at a flaw radius  $r$  and with a surface energy  $\gamma$  and

$$\frac{4}{3}\pi r^3\sigma = 4\pi r^2\gamma \text{ which implies a defect scale of order } \frac{\gamma}{\sigma} \text{ in an isotropic metal.} \quad (2)$$

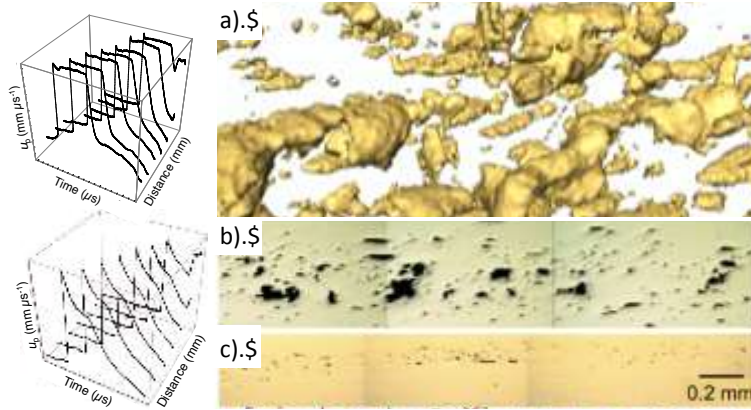


**FIGURE 3.** Ductile void growth in a stainless steel. Typical particle velocity histories for square and triangular waves (left). Right; a). X-ray tomographic image of ductile spall voids. b). equivalent section of the void distribution from the same target, c). effect of triangular pulse at the same stress magnitude on the void distribution.

Typical values for water give cavity sizes of order 10 nm. For a brittle ceramic such as alumina the flaw size rises to *ca.* 100 nm. Of course fracture occurs at the brittle mesoscale glass grain boundaries since the sapphire grains are an order of magnitude stronger. Surface energies for metals are typically of order 1  $\text{J m}^{-2}$  and this magnitude results in small critical flaw sizes. However Irwin, during the second war, showed that the level of energy needed to cause ductile fracture is an order of magnitude higher than the corresponding surface energy, and that plastic work must be taken into account. The behaviour is not elastic and stress concentrations are diffused away from the flaw under these conditions. Thus a realistic energy is of order 1000  $\text{J m}^{-2}$  which gives a minimum void size of *ca.* 1  $\mu\text{m}$ . It will be noticed that iron in particular requires a defect of orders of magnitude greater size than that in copper to form a cavity and so fracture is favoured in BCC iron over void formation as in the case of FCC copper. This is shown graphically in the sectioned spall planes recovered from a commercially pure copper and Armco iron (Fig. 2).

In a recent study on the shock properties of stainless steel subject to square and triangular profile pulses, recovered targets were analysed and void volume was investigated using X ray tomography [11]. Incipient failure of the metal induced by each pulse type displayed characteristics that could be quantitatively assessed using

tomographic reconstructions. In the case of the triangular pulse the tensile loading time was greatly reduced relative to that from the interacting release fans in the square profile experiment by reflection from a rear surface, not by interaction of propagating releases. A void field from a square topped pulse is shown in Fig. 3 a). The cavities show varying size and in the central region where the release fans have crossed they have coalesced to form contiguous connected volumes with features perpendicular to the shock direction. In b) a section of the steel is shown and in c) that through a target subject to a tensile pulse at the same peak compressive stress is shown for comparison. The void size distributions for the two cases show a cut off in the diameter for the voids that are produced of 1  $\mu\text{m}$  which is the lower boundary for void formation derived in (2) above for this material. This threshold indicates critical work done within a volume in a particular metal where it is favourable to form a void and create a mesoscale defect within the microstructure.

Finally recent work has illustrated a second level of detail in the nucleation of voids occurring at mesoscale grain boundaries. Escobedo *et al.* have shown that grain misorientation favours nucleation at particular boundary types by loading well-characterized OFHC Cu samples with various grain sizes subjected in uniaxial strain [12]. They noted both the integrated spall strengths determined from the reflected wave from the spall plane, and recovered targets for microstructural examination and characterization of damage with respect to the grain orientations.

The spall strength from free surface velocimetry (VISAR) showed no change with variations in grain size however the damage states were different in a series of cases. There was a critical length scale for transition from a regime in which nucleation dominated the observed response to a case where voids had grown significantly and dominated recovered targets. The results show that for samples with small (30  $\mu\text{m}$ ) and large (200  $\mu\text{m}$ ) grain sizes the growth of voids is dominated by coalescence, whereas for medium (60  $\mu\text{m}$  and 100  $\mu\text{m}$ ) grain sizes the growth is restricted to a much slower process of individual void growth. Electron backscatter diffraction (EBSD) reveals that voids preferentially nucleate at grain boundaries with high misorientation angles while special boundaries (low angle  $\Sigma 1$  and high angle  $\Sigma 3$ ) proved to be more resistant to void nucleation. Orientation of grains will offer differing slip systems to the metal to allow cavitation to proceed affecting the rate and nature of the nucleation of damage that is recorded.

That spall strength remains comparable in all these experiments is confirmation that these mesoscale differences in behavior are mediated at greater length scales so that momentum is conserved and the failure zone across the target will have the same work done within it regardless of the details observed. Yet within the weak shock regime the micromechanics of failure occurs at inhomogeneities during damage in the material. Microstructural length scales dictate the growth mechanism (coalescence or individual void growth) and the damage rate (kinetics) that results in the observed particle velocity histories at the target scale. The dependence of nucleation on grain orientation confirms that stacking defects are a potent means of stress concentration where failure can nucleate [12]. Failure is a mesoscale consequence of component scale loading and localization where tensile pulses can span volumes encompassing weak grain boundaries within the microstructure where grain boundaries fails.

### 2.3 Defect evolution with time and scale

The previous section has illustrated the evolution of localized failure from nucleation at the microscale to a mesoscale surface that will grow as the pulse progresses. Nucleation in the weak shock regime begins when stress concentrations allow plastic work to dissipate at critical defects and propagate failure from this populations of sites. Further the formation of ductile voids during tensile failure occurs more easily in FCC than BCC metals since the former have both lower Peierls stresses, higher stacking fault energies and indeed lower surface energies once a volume has failed. Before the compressive stress has reached the WSL (where all crystals and flaws are activated and the flow is homogeneous) localization occurs in a population at the microscale that grows to fail regions at the mesoscale. Finally when the amplitude and duration of the tensile impulse are both sufficient, incipient voids coalesce and a damage plane opens that conserves momentum to ensure Newton's laws are obeyed.

It is of course both amplitude and duration in the tensile pulse that cause failure within materials. Longer pulses can sample a larger range of defects at the microscale, mesoscale and even joints within structures if the loading pulse is long enough. When the duration grows too short, the pulse's ability to sample an assemblage of grains at the mesoscale is reduced and instead samples a range of volume defects within the grain at the microscale. The critical pulse length that crosses from meso- to microscale is of order of magnitude 10 ns for a nominal polycrystalline metal. This means that different loading platforms will effectively sample single crystal or bulk properties yielding greatly differing results for measured tensile strengths as one moves from the mesoscale to single crystal measurements [7]. In Fig. 3 the response of a stainless steel to short as opposed to long pulse loading is presented. A

triangular pulse can only nucleate and grow a small number of smaller voids compared with the square pulse at the same amplitude which can nucleate and grow many larger ones as has been documented. However the impulse itself ( $\int F dt$ ) is much less for a triangular than a square pulse equivalent. In fact a separate experiment was done in that series that took material to a higher triangular pulse amplitude but kept the impulse *matched* to the initial square pulse. In that case the pull back signal and total void volume were matched but the void morphology was very different since the total integrated time under stress of the cavitation process was not.

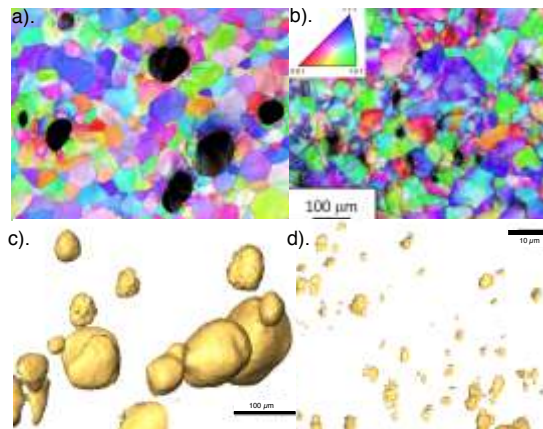


**FIGURE 4.** EBSD maps of: (a) 10.6 GPa loaded Ta sample showing well-formed elliptical voids with few localization linkages. (b) Secondary spall plane in the 10.6 GPa sample showing localized plasticity vortices within grains serving as nucleation sites for incipient voids. (c) XCT imaging of the voids in (a) and (d) the voids in (b) showing only open new free surface.

A second example is shown in Fig. 4. Here targets were prepared from commercially pure, annealed BCC tantalum plate. The average grain size was  $35 \mu\text{m}$  in this material. Once shocked, targets were interrogated dynamically using Photon Doppler Velocimetry (PDV) and recovered for post-mortem analysis using X ray computed tomography (XCT) [13]. The sample shows incipient spallation. It was loaded to 10.6 GPa peak stress and the target possessed two incipient damage fields seen using EBSD (a and b) and XCT of the voids (c and d). A field of isolated  $50$  to  $100 \mu\text{m}$  diameter voids is seen in Fig. 4 a) and c) and a secondary field of numerous small ( $<50 \mu\text{m}$ ) sites is shown in Fig. 4 b) and d). The primary damage field with the larger voids contains few linking localizations but has some isolated fine twins and intragranular lattice rotations of up to  $35^\circ$  in grains adjacent to the voids. The secondary damage field displays more extensive work done throughout the region with most grains affected by some deformation, no evidence of twinning, extensive strain near grain boundaries, and intragranular lattice rotations across the region of *ca.*  $35^\circ$ . In this one target, these two planes show void nucleation and growth processes to be operative within the metal. The images in b) and d) show an anisotropic distribution of dislocation slip bands and localized shear features all located at or near grain boundaries; the preferred nucleation sites for incipient spall in these nominally 1D experiments. Tomography measures void volume fractions to be 1.23% and 0.08% within the developed and the nucleating spall planes respectively. In the early stages of deformation, planar features at the weakest planes are nucleated within the target with the short pulse loading applied. Once the surfaces have opened sufficiently that cavitation can occur, voids grew preferentially from a small selection of these sites creating new free surface whilst the pulse is applied.

The observation of damage nucleation leading to voids located at grain boundaries shown above is in contrast to void formation occurring preferentially at deformation twin-twin or at twin-grain boundary intersections in Ta shocked via a sweeping detonation wave [14]. In this case increased shear and shortened pulse length contribute to activate further nucleation of damage within the tantalum. Thus the behaviour seen in this loaded tantalum shows many features of the global process not previously seen in other experiments. The first moments show global microstructural response with plastic deformation in grains contributing to the opening of a population of nucleation sites failing grain and twin boundaries to create a mesoscale damage state. With time this evolves to a few large spherical voids in which the plastic work imparted in the tensile pulse is expended and steady growth of these occurs until coalescence and macroscopic failure occurs across the plane over which the tensile pulse was first located. The beginning of failure in the weak shock regime is progressive damage at grain boundaries at the microscale leading to the development of the defect field into a steady growth of large cavities at the mesoscale which coalesce and fail the material at later times at the macroscale.



Thus there are changes in the observed final microstructure that stem from changes in the applied tensile pulse which result in differing measured material strengths from the operating damage kinetics [7]. Fig. 5 a) shows the variation of yield stress with pulse length (calculated from the strain rate data) for four materials tested on different platforms; a polymer, an FCC and a BCC metal and a polycrystalline ceramic. Fig. 5 b) shows variation of tensile stress with pulse length for pure aluminium; a high SFE-FCC metal. As will be seen from the figure, the shortest pulse times sample the highest strengths which occur in the regimes where loading pulses are shorter than *ca.* 200 ns in a) and 10 ns in b). The shock pulse probes a spatial extent with a defect population accessed by it. Compressive strength increases when there are no grain boundaries and loading is within a single crystal. When the pulse is longer the strength drops as the mesoscale defect population is sampled. For tensile pulses of duration less than 10 ns where no grain boundaries are sampled, spall strength rises rapidly towards the theoretical strength  $E/2\pi$  (*ca.* 10 GPa for this metal) as the pulse length decreases. Other work has shown a change in deformation mechanisms as the pulse length drops. Voids are no longer found when the pulse cannot do enough work to create a new free surface and experimental work with laser spall has shown only ductile fracture on the surfaces recovered and examined [15].

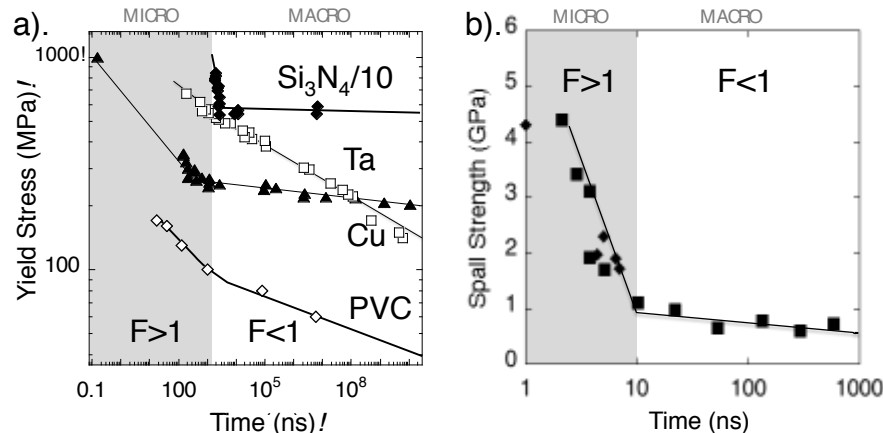


**FIGURE 5.** Compressive, a), and tensile, b), loading of materials. In a) the variation of flow stress with pulse length is shown for PVC, Cu, Ta, and Si<sub>3</sub>N<sub>4</sub>. In b) the variation in spall strength with pulse length is shown for a pure aluminium from various studies [7]. The diamond on the ordinate marks the theoretical shear strength for the material.

When the amplitude of these pulses approaches the bond strength of the metal, failure occurs within a homogeneous plane with deformation localized at a fixed position defined by the geometry of the event that instigated the pulse. Of course a compression pulse may load and then be reflected to induce damage as discussed earlier and in that case, if the compression were above the WSL, volume defects within the grains would be eliminated within the shock front. However grains themselves would not reorient and so stacking defects would remain after release at the locations of the original grain boundaries. As in the case of the sweeping detonation these would act as potent sources of failure within the lattice with nucleation at these large misorientations between the grains within the solid [14].

### 3. DISCUSSION AND CONCLUSIONS

Tensile failure is a matter of conserving momentum and energy as found in regimes of material behavior where the tensile stress is greater than the bond strength or when failure is entirely brittle so that it is pseudo-instantaneous. However when material strength becomes significant there is a response where some microstructure yields while some remains elastic and plastic work is localized at particular sites. The challenges of theory and experiment in this inhomogeneous regime make prediction of complete failure difficult since there is no single threshold and material may be left intact but with internal damage that is only possible to predict statistically. These features are exemplified by the shock response of ductile metals in the weak shock regime.

Failure occurs primarily by only one of two mechanisms; nucleation and growth of ductile voids or nucleation of cracks and failure by fracture from critical defects. In either case the two step process means that pulses can be used to filter mechanisms either by activating mechanisms by exceeding relevant stress thresholds or by fixing impulse duration to adjust for the timescale of one process or the other. In the incipient case when damage is activated but doesn't complete, the most interesting case will be when a defect nucleates ductile failure and surface energy is liberated to form an opening void. These processes take time and depend on the slip systems for the metal as has

been seen. However in the initial nucleation phase the failure is always by fracture at the microscale. In a brittle material the process is normally fast and completes once the crack has been nucleated since its propagation liberates energy. In ductile materials there comes a point in the opening planes where the work done can generate a new surface and a void can grow defining a mesoscale object in the flow. These opening voids have competing strain fields that interact and whilst some continue to propagate, others are arrested. At later times the localization is complete and void growth proceeds until coalescence links cavities and fails a free surface at the macroscale. Thus processes run forward from nucleation with planar failure at the earliest times to ductile plasticity later once surface has been created. Short impulses are confined to ductile fracture as seen in targets recovered from laser-loaded metals.

Whilst all of these features are seen in crystalline solids, only fracture can nucleate within an amorphous material since there are minimal mechanisms available for plasticity that can localize in any other manner. Glass offers a simple illustration of the accommodation of failure in an amorphous solid. The compression of glasses can only proceed by fracture that occurs from volume defects within the glass. Most of these lie on the surface of a glass block. In the strong shock regime above the WSL for the glass the material behaves in a simple manner and fractures behind a shock front that shows zero strength when it is probed by a tensile pulse after loading. There is a regime before this limit where fracture driven from the surface defects cannot travel at the speed of the elastic wave in the glass. The material thus displays differing spall strengths behind the shock in the unfailed material where it retains strength or behind the failure front which follows. Thus in this weak shock regime the strength of the glass is determined by position and time into the loading as is seen by ductile materials with more additional deformation mechanisms.

In the first instance simple hydrocode models use a simple approach that assumes that computational cells fail when the pressure falls below a minimum level  $P_{\min}$ . This approach is valid if the criterion is applied only in the homogeneous regime above the WSL. However once failure occurs in a regime where microstructure sees localization and partial damage is not unique, no simple single parameter model will ever reproduce inhomogeneous failure in detail, let alone be predictive in any quantitative manner. However as microscale failure transits to mesoscale plasticity there is a change to void formation at critical thresholds for creation of new free surface. Further mesoscale voids link to form macroscale fracture surfaces at later times. This nested suite of microscale/mesoscale/macroscale deformation mechanisms can be implemented in models particularly if they run on new parallel platforms and perhaps these offer the best means of treating failure in these ductile materials for the future. Accordingly it may become possible to treat defect activation taking account of grain orientation, defects within the substructure, twin boundaries with significant shear in the initial loading and other means that will localize strain for the requisite amount within the lattice. Once all of these processes have been considered, only then will one decide between fracture and plasticity from the defect under load.

In the final reckoning the regime in which loading occurs between the elastic limit and where the stress can overcome the theoretical strength of the material is a complex inhomogeneous composite of states in which a unique solution to a material response is difficult to extract. Yet one can always say that Newton's laws are obeyed and that the material will take the simplest route to conserve the momentum supplied by the impulse with which it interacts.

## ACKNOWLEDGMENTS

We thank all the colleagues who contributed to the work presented in this paper in Manchester and Los Alamos including S.A. McDonald, P.J. Withers, E.K. Cerreta, V. Livescu, C.P. Trujillo and J.C.F. Millett.

## REFERENCES

1. Tresca, H., *Proc. Inst. Mech. Engrs*, **30**, 301 (1878).
2. Hopkinson, J., *Proc. Manch. Liter. Philos. Soc.*, **11**, 40 (1872).
3. Massey, H. F., *Proc. Manchester Assoc. Engrs*, 21 (1921).
4. Hopkinson, B., *Proc. R. Soc. Lond. A.*, **89**, 612, 411-413, (1914).
5. Hopkinson, B., in *The Scientific Papers of Bertram Hopkinson*, edited by J. A. Ewing and J. Larmor (Cambridge University Press, Cambridge, 1921), 423.
6. Bourne, N. K., *Materials in Mechanical Extremes: Fundamentals and Applications*, Cambridge: Cambridge University Press, (2013).
7. Bourne, N. K., *Metallurgical and Materials Transactions A.*, **42A**, 2975 (2011).
8. Brennen, C. E., *Cavitation and Bubble Dynamics*. Oxford University Press, New York, (1995).

9. Boteler, J. M. and Sutherland, G. T., [J. Appl. Phys.](#) **96**, 6919 (2004).
10. Curran, D. R., Seaman, L. and Shockey, D. A., Dynamic failure in solids, [Phys. Today](#), **30**: 46 (1977).
11. Gray III, G. T., Bourne, N. K. and Henrie, B. L., [J. Appl. Phys.](#) **101**, 093507 (2007).
12. Escobedo, J. P., Cerreta, E. K., and Dennis-Koller, D., [JOM](#), **66**, 156 (2014).
13. Gray III, G.T., Bourne, N.K., Livescu, V., Trujillo, C., MacDonald, S., Withers, P.J. Phys: Conf. Ser. **500** 112031 (2014).
14. Gray III, G., Hull, L., Livescu, V., Faulkner, J., Briggs, M., Cerreta, E., [EPJ Web of Cons](#), **26**, 02004 (2012)
15. Jarmakani, H., Maddox, B., Wei, C. T., Kalantar, D., and Meyers, M. A., [Acta Materialia](#) **58**, 4604 (2010).